Effect of Sensitizer Protonation on Singlet Oxygen Production in Aqueous and Nonaqueous Media

Jacob Arnbjerg,[‡] Mette Johnsen,[‡] Christian B. Nielsen,[†,‡] Mikkel Jørgensen,[†] and Peter R. Ogilby*[,‡]

Department of Chemistry, University of Aarhus, DK-8000, Århus, Denmark, and Polymer Department, Risø National Laboratory, DK-4000, Roskilde, Denmark

Received: October 18, 2006; In Final Form: January 24, 2007

The yield of singlet molecular oxygen, $O_2(a^1\Delta_g)$, produced in a photosensitized process can be very susceptible to environmental perturbations. In the present study, protonation of photosensitizers whose chromophores contain amine functional groups is shown to adversely affect the singlet oxygen yield. Specifically, for bis-(amino) phenylene vinylenes dissolved both in water and in toluene, addition of a protic acid to the solution alters properties of the system that, in turn, result in a decrease in the efficiency of singlet oxygen production. In light of previous studies on other molecules where protonation-dependent changes in the yield of photosensitized singlet oxygen production have been ascribed to changes in the quantum yield of the sensitizer triplet state, Φ_T, and to possible changes in the triplet state energy, E_T, our results demonstrate that this photosystem can respond to protonation in other ways. Although protonation-dependent changes in the amount of charge-transfer character in the sensitizer-oxygen complex may influence the singlet oxygen yield, it is likely that other processes also play a role. These include (a) protonation-dependent changes in sensitizer aggregation and (b) nonradiative channels for sensitizer deactivation that are enhanced as a consequence of the reversible protonation/deprotonation of the chromophore. The data obtained, although complicated, are relevant for understanding and ultimately controlling the behavior of photosensitizers in systems with microheterogeneous domains that have appreciable pH gradients. These data are particularly important given the use of such bi-basic chromophores as two-photon singlet oxygen sensitizers, with applications in spatially resolved singlet oxygen experiments (e.g., imaging experiments).

Introduction

Singlet molecular oxygen, $O_2(a^1\Delta_g)$, is a reactive species that plays a role in many chemical and biological processes.[1] Singlet oxygen is particularly important in mechanisms by which cellular function is altered in both plant[2,3] and animal[4,5] systems. Indeed, the presence of singlet oxygen can result in cell death, a phenomenon that forms the basis for photodynamic therapy, PDT, which is a medical treatment used to destroy undesired tissue (e.g., cancerous tumors).[6]

Singlet oxygen is commonly generated by irradiation of a molecule, a photosensitizer, that is either endogenous (e.g., chlorophyll in a plant cell) or is specifically added to the system of interest (e.g., a drug for PDT).[7] In this process, energy transfer to ground state oxygen from an excited electronic state of the photosensitizer, generally the lowest excited triplet state, results in the production of singlet oxygen.

When discussing the photosensitized production of singlet oxygen, it is usually implied that sensitizer excitation occurs in a linear, one-photon process. It is now well established, however, that singlet oxygen can also be efficiently produced upon the nonlinear, two-photon excitation of a sensitizer.[8−14] Given the comparatively rapid processes of intramolecular relaxation that occur after photoexcitation, it is assumed that the excited electronic state that is ultimately quenched by oxygen to produce singlet oxygen is the same upon both one- and two-photon excitation of the sensitizer.[8] In both cases, phenomena that perturb the photophysics of the sensitizer can be reflected in the production of singlet oxygen.

For the present study, we are interested in the effect of sensitizer protonation on the photoinduced production of singlet oxygen. Many singlet oxygen sensitizers have an amine-based functional group judiciously placed on the chromophore which, in turn, provides a site that is readily perturbed by protonation. Indeed, for the specific case of two-photon sensitizers,[9,11] and for a wide range of molecules in general,[15−18] electron-donating amino groups on the chromophore can result in comparatively large two-photon absorption cross sections.

For this work, we have chosen to examine the effect of protonation on the yield of singlet oxygen sensitized by the amino-substituted phenylene vinylenes shown in Chart 1. The first molecule, (*E*,*E*)-2,5-dibromo-1,4-bis[2-(4′-dimethylaminophenyl)vinyl]benzene, DMAPV, is readily soluble in toluene. For the second molecule, (*E*,*E*)-2,5-dibromo-1,4-bis[2-(4′-dimonomethylether triethylene glycol aminophenyl)vinyl]benzene, MTEGPV, the monomethylether triethylene glycol units render this chromophore soluble in a variety of solvents, including water and toluene.

It has been demonstrated that this general class of molecules can have comparatively large probabilities for two-photon absorption.[18] We have also used such amino-substituted molecules as two-photon singlet oxygen sensitizers in both aqueous and nonaqueous media.[8−12] One goal in our work is to develop

* To whom correspondence should be addressed. E-mail: progilby@chem.au.dk.
† Risø National Laboratory.
‡ University of Aarhus.

10.1021/jp066843f CCC: $37.00
Published on Web 05/05/2007

CHART 1

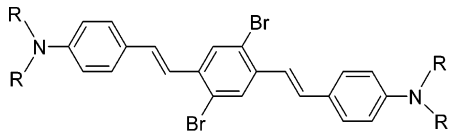

$R = CH_3$ **DMAPV**

$R = (CH_2CH_2O)_3CH_3$ **MTEGPV**

sensitizers that can be used in two-photon-based, spatially resolved singlet oxygen experiments (e.g., imaging experiments in biological samples).[19−21] For the present, however, DMAPV and MTEGPV simply provide a vehicle to explore the effects of protonation on the photosensitized yield of singlet oxygen. Related amines have recently been used by Werts et al.[22] to study the effect of protonation on two-photon excited fluorescence.

With reference to our imaging work, we are particularly interested in examining the effect of protonation in both hydrophobic and hydrophilic systems. The study of protonated species in hydrophobic media can be nontrivial and depends critically on the acid used. Although many protic acids are soluble in a solvent such as toluene, the protonation of a base in this solvent often results simply in the formation of an insoluble salt. For many systems, however, including those studied here, trifluoroacetic acid (TFA) can be used to protonate an organic amine in toluene, and the resultant ion pair will remain in solution. As such, we set out to examine the behavior of DMAPV and MTEGPV in both toluene and water solutions using, as our acid of choice, TFA.

Background. There are many systems of both fundamental and practical importance in which local concentrations of protons vary. Because of their prevalence, biological systems provide important examples. There have also been many attempts to assess the influence of protonation on the behavior of a singlet oxygen sensitizer. Summarizing certain aspects of this previous work is useful, not just to put our own work into perspective but to establish a more coherent framework for a complicated problem.

It has been established that pH can influence the extent to which certain sensitizers are incorporated and retained in a cell.[23−25] Likewise, the extent to which a sensitizer is protonated can influence where it tends to localize in specific subcellular domains (e.g., hydrophilic vs hydrophobic domains).[26] In turn, the microenvironment of a given domain could influence singlet oxygen yields in a number of ways. For example, it has been shown that a bacteriopheophorbide generates singlet oxygen with unit quantum efficiency in organic solvents, whereas at the hydrocarbon−water boundary in aqueous micellar systems, electron transfer from the triplet sensitizer to oxygen competes to decrease the singlet oxygen yield.[27] The local solvent environment could also promote sensitizer aggregation, a phenomenon known to result in decreased yields of singlet oxygen.[28] Thus, in a biologically relevant heterogeneous system, the pH-dependent spatial distribution of a sensitizer could indeed influence the photoinduced concentration profile of singlet oxygen.

Of course, protonation of a sensitizer may not only influence the spatial domain in which the molecule tends to localize, but it may also have a more direct effect on the photophysics of the chromophore. This is an equally important phenomenon with many ramifications. For example, given that the production of singlet oxygen in or near the mitochondria is important in mechanisms of cell death,[29] and that pH gradients exist around this organelle,[30] protonation-dependent changes in the chromophore could either impede or accelerate cell destruction. Spatial domains around cancer cells are also characterized by unique pH gradients,[31,32] and such local differences in proton concentration could certainly influence the effectiveness of sensitizers administered as drugs in PDT.[25,33]

Surprisingly, there is not as much information available as one might perhaps expect on the effect of pH on the photosensitized production of singlet oxygen. Moreover, for the data that are available, the influence of pH seems to be molecule specific with little evidence of systematic trends.

One of the earliest studies of substance was performed in the mid-1970s. In this work, the effect of pH on the oxygen-dependent photophysics of thiazine dyes, in particular, methylene blue, was examined.[34−36] Upon acidification of this system, protonation occurs at an unsaturated nitrogen atom that is an intrinsic part of the sensitizer chromophore. A decrease in the yield of singlet oxygen in more acidic solutions was correlated to the observation that the rate constant for oxygen quenching of the triplet state of protonated methylene blue was significantly smaller than that for the unprotonated triplet state. This difference in rate constants was said to reflect differences in the energies of the corresponding triplet states [i.e., E_T(protonated) < E_T(unprotonated)], with E_T(protonated) having been estimated to be very close to the excitation energy of singlet oxygen, 94 kJ/mol. It was argued that, under these latter conditions, reversible energy transfer between singlet oxygen and the sensitizer triplet state could be manifested in a smaller rate constant for quenching by oxygen.

In a study arguably related to that of the thiazine dyes, it has been shown that protonation of the azomethine bridging nitrogens of the phthalocyanine macrocycle likewise results in a pronounced decrease in the yield of singlet oxygen produced in a photosensitized process.[37,38] In the interpretation of these data, it was also suggested that successive protonation results in a decrease of the triplet energy, ultimately resulting in a situation where the production of singlet oxygen is energetically not feasible. However, in apparent contrast to these phthalocyanine data, protonation of the nitrogens in the macrocycle of water-soluble *meso*-tetraphenylporphyrin and *meso*-tetrapyridylporphyrin derivatives does not result in an appreciable change of the singlet oxygen yield.[26,39] In a follow-up to one of these latter studies, Kruk and Braslavsky showed that if, instead of the porphyrin, one uses the corresponding dihydroporphyrin (i.e., the chlorin) in which one of the pyrrole rings in the macrocycle has been reduced, then protonation of the nitrogens in the macrocycle does have a pronounced adverse effect on the yield of singlet oxygen.[40] This difference in behavior between the porphyrin and the chlorin was attributed to an increased conformational flexibility in the macrocycle of the chlorin which, upon protonation, facilitates an increase in the rate of $S_1 \rightarrow S_0$ radiationless deactivation.[40] The latter adversely influences the yield of the chlorin triplet state which, in turn, is manifested in a lower yield of singlet oxygen.

Ostler et al.[41] have observed that changes in pH likewise influence singlet oxygen production when the sensitizer is a sulfonated aluminum phthalocyanine. In this case, a decrease in the singlet oxygen yield with an increase in the acidity of the solution was attributed to a ligand-dependent change in the extent of sensitizer dimerization. Specifically, upon protonation, a ligand-bridged phthalocyanine dimer forms, which, compared to the phthalocyanine monomer, does not produce singlet oxygen in appreciable yield.

In other work, it has been shown that, in alkaline solutions, deprotonation of hydroxyl groups in the sensitizer hypericin results in an appreciable decrease in the yield of the triplet state [i.e., $\Phi_T(\text{hypericin}-H_2) = 0.71 \pm 0.05 \rightarrow \Phi_T(\text{hypericin}^{2-}) < 0.05$].[42] In turn, this is reflected in a corresponding decrease in the hypericin-sensitized yield of singlet oxygen.[42,43] Conversely, for pterin derivatives, a slight increase in the quantum yield of singlet oxygen production as the system was made more alkaline has been reported.[44,45] In this case, where the acid−base equilibrium involves an amide group (neutral protonated form) and a conjugated enolate (deprotonated form), one may infer from the data that the singlet oxygen yields likewise reflect pH-dependent changes in the efficiency with which the triplet state pterin is produced.

Implicit in the examples cited thus far is the notion that changes in pH directly influence the sensitizer chromophore. As such, pH-dependent changes in the yield of singlet oxygen are generally accompanied by noticeable pH-dependent changes in the absorption and fluorescence spectra of the sensitizer. On the other hand, it is possible to have a pH-sensitive functional group (e.g., an amine) covalently attached to the sensitizer in such a way that it is not part of the chromophore. In this case, one could envision a scenario where the effects of protonation could be indirectly manifested in the behavior and properties of the chromophore. Indeed, McDonnell et al.[46] have recently provided a nice example of such a system. In the free base, electron transfer from the amine to the excited-state chromophore obviates the production of singlet oxygen. Upon protonation of the amine, however, electron-transfer quenching of the chromophore is precluded, and singlet oxygen production can ensue. In this same vein, it has been shown that, in 2-arylpropionic acid sensitizers, pH-dependent photodecarboxylation reactions can compete with the process of energy transfer to oxygen and thus adversely affect the yield of singlet oxygen.[47]

In closing our summary of the published literature, it is pertinent to at least mention the arguably related effect of pH on the efficiency with which a given molecule can quench singlet oxygen.[48−50] Of course, once singlet oxygen has been formed in a given system, any pH-dependent change in the rate with which it is removed could likewise be manifested in a process such as cell death. From a more fundamental perspective, however, it is important to recall that the photosensitized production of singlet oxygen and the quenching of singlet oxygen both involve transitions between states of an oxygen−organic molecule encounter complex.[7,51,52] As such, one can easily find common ground to study the effect of protonation on these separate phenomena.

Experimental Section

Instrumentation. Absorption spectra were recorded using a Hewlett−Packard model 8453 diode array spectrometer. Steady-state fluorescence measurements were performed using Perkin Elmer (LS45) and Horiba Jobin Yvon (Fluoromax P) fluorometers. Time-resolved fluorescence measurements were made using a home-built, time-correlated single-photon counting apparatus (based on Becker & Hickl components, 200 ps rise time). Fluorescence quantum yields were determined using 9,10-diphenylanthracene in cyclohexane as the standard ($\Phi_F = 0.93 \pm 0.03$),[53] with corrections made for differences in the refractive index of the solution.

Singlet oxygen quantum yields, Φ_Δ, were determined using instruments and an approach that has been previously described.[8,54] For these measurements, the sample was irradiated at either 355 nm (third harmonic of a nanosecond Nd:YAG pulsed laser) or at 416 nm. The latter wavelength was obtained using a home-built H_2 Raman shifter in which the first Stokes line of the 355 nm source was isolated. The standard used for experiments performed in toluene was phenalenone ($\Phi_\Delta = 1.00 \pm 0.05$),[55] whereas the 2-sulfonic acid derivative of phenalenone was used as the standard for experiments in water ($\Phi_\Delta = 0.97 \pm 0.06$).[56]

SCHEME 1

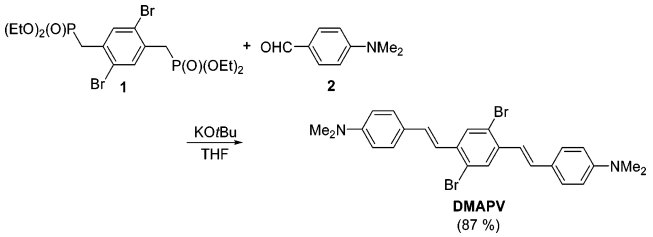

Time-resolved triplet absorption and laser-induced optoacoustic calorimetry (LIOAC) measurements were made using instruments and approaches that have likewise been previously described.[8,12]

Materials. Toluene, $CHCl_3$, and THF (Sigma-Aldrich, spectroscopic grade), anisole (Sigma-Aldrich, >99%), 1,4-dioxane (Rathburn, HPLC Grade), 1-propanol (Merck, analytical grade), and trifluoroacetic acid and 2-hydroxybenzophenone (Sigma-Aldrich, 99%) were used as received. Water was triply distilled, while experiments in deuterated water were performed using fresh batches of D_2O (99.9%, Eurison Top) in order to minimize hydrogen exchange. Samples for measurements performed in the absence of oxygen were prepared by gently bubbling solvent-saturated nitrogen through the solution for approximately 15 min.

Sensitizer Preparation. The synthesis and characterization of MTEGPV has been published.[10] DMAPV was prepared using the procedure outlined in Scheme 1. For this procedure, the precursor phosphonic acid ester, [2,5-dibromo-4-(diethoxyphosphorylmethyl)benzyl] phosphonic acid diethyl ester, **1**, was prepared using an approach that has been published.[57] A solution of **1** (0.34 g, 0.63 mmol) and 4-(dimethylamino) benzaldehyde (0.56 g, 3.8 mmol), **2**, was then prepared in 50 mL of THF. KO*t*Bu (0.54 g, 4.8 mmol) was then added, and the reaction mixture was refluxed for 30 min. After cooling to room temperature, the mixture was quenched with 50 mL of 2 M HCl, and the organic phase was isolated. Removal of the solvent left a solid material which was recrystallized from a mixture of THF/ethanol to yield 0.29 g (87%) of DMAPV as a red powder; mp: 273−275 °C. ^{1}H NMR ($CDCl_3$): 7.83 (s, 2H), 7.45 (d, 4H, $J = 9$ Hz), 7.17 (d, 2H, $J = 16$ Hz), 6.98 (d, 2H, $J = 16$ Hz), 6.74 (d, 4H, $J = 9$ Hz), 3.01 (s, 12H). ^{13}C NMR ($CDCl_3$): 150.5, 137.1, 131.8, 129.6, 128.1, 125.0, 122.6, 121.3, 112.2, 40.4. Anal. Calcd for $C_{26}H_{26}Br_2N_2$: C, 59.33; H, 4.98; N, 5.32. Found: C, 59.43; H, 4.95; N, 5.35.

Results and Discussion

pH-Dependent Spectral Changes. DMAPV is not soluble in water, and as such, our photophysical measurements with this sensitizer were performed in toluene. For this study, we do not use the pH scale which derives from the concentration of dissociated protons. Rather, we refer to the amount of TFA added to toluene solutions of DMAPV.

In toluene, DMAPV has an absorption band with λ_{max} at ~416 nm (Figure 1). Upon successively increasing the amount of added TFA, the intensity of this absorption band decreases, and other bands appear in the region of ~300−370 nm

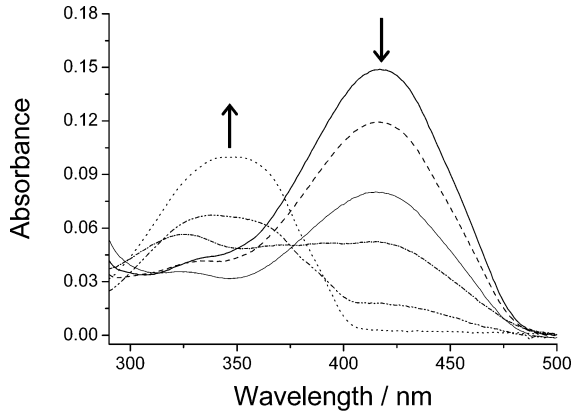

Figure 1. Absorption spectra of DMAPV in toluene containing different amounts of trifluoroacetic acid, TFA. The spectra shown reflect different molar ratios of TFA to DMAPV, expressed as $\log(n_{TFA}/n_{DMAPV})$: (—), no TFA; (- - -), 1.5; (—), 1.9; (- • - • - •), 2.5; (- •• - •• - ••), 2.9; (• • •), 3.5. Arrows indicate the direction of change in the spectra upon adding increasing amounts of TFA.

(Figure 1). At a sufficiently high amount of added TFA, one observes a single absorption band with λ_{max} at ~350 nm.

Under the conditions employed in our experiments, TFA itself does not absorb at wavelengths longer than 300 nm. Thus, the data are consistent with the production of more than two TFA-dependent species, and this is supported by the lack of an isosbestic point in the spectra recorded. With two basic sites in DMAPV, one might expect to have a TFA concentration-dependent equilibrium between three species, DMAPV, DMAPV$-H^+$, and DMAPV$-H_2^{++}$. Of course, in toluene, it is expected that the trifluoroacetate counterion would be intimately associated with the protonated amines, and this, in turn, would be reflected in the spectra recorded. To further examine this latter phenomenon, we monitored the effect of using an acid other than TFA.

Upon the addition of methane sulfonic acid, CH_3SO_3H, to a toluene solution of DMAPV, we likewise observed a decrease in the intensity of the absorption band with λ_{max} at ~416 nm. Although another blue-shifted band correspondingly appeared with the addition of CH_3SO_3H, it was much broader and had a peak maximum (~330 nm) at a shorter wavelength than the band ultimately observed in the TFA experiment. As with the TFA system, an isosbestic point was not observed in the spectra recorded upon CH_3SO_3H addition. Although these data are consistent with the expectation that, upon the addition of the acid, the spectra observed should partly reflect the nature of the counterion, some caution should nevertheless be exercised. Specifically, for the TFA system, we never observed the formation of a precipitate and could always reproduce the spectra shown in Figure 1. For the CH_3SO_3H system, however, we occasionally saw the formation of small crystals, indicating that the ion pair was not particularly soluble and that light scattering likely contributed to the spectra recorded. When benzene sulfonic acid was used as the proton source for a DMAPV experiment in toluene, the ion pair clearly precipitated out of solution. All of these effects, as manifested in the observed spectra, were reversible upon the addition of $N(CH_3)_3$ to each of the acid-containing solutions.

To further extend our studies, we investigated the structurally similar compound MTEGPV in both toluene and water. Although the concept of pH is well-defined in water, we still refer to the amount of added TFA for the sake of consistency. Nevertheless, we independently ascertained that, based on the amount of TFA added, the calculated value of the pH (e.g., at

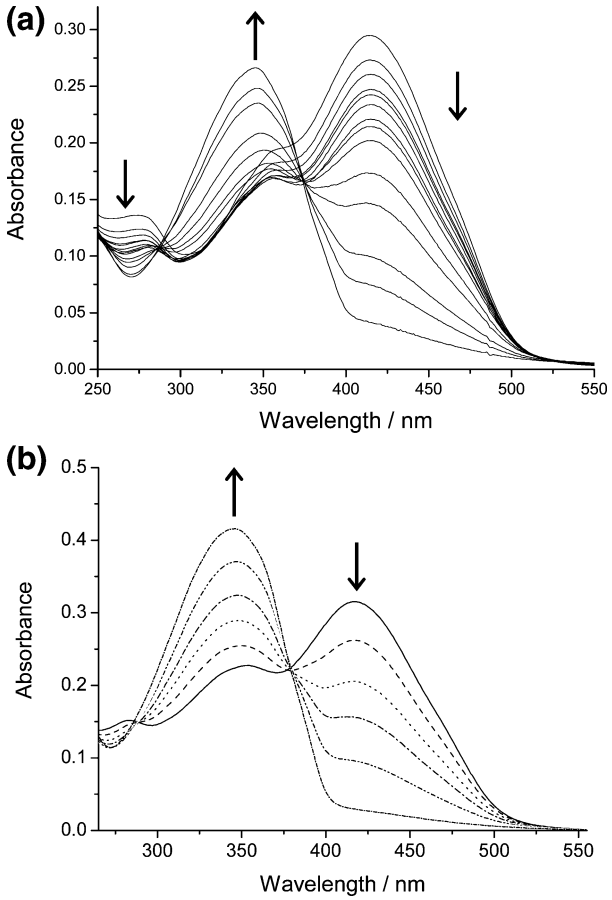

Figure 2. Absorption spectra of MTEGPV in water containing differing amounts of trifluoroacetic acid, TFA. The spectra shown reflect different molar ratios of TFA to MTEGPV. (a) Spectra recorded under conditions that range from no added TFA to $\log(n_{TFA}/n_{MTEGPV}) > 3.4$. (b) Selected spectra where $\log(n_{TFA}/n_{MTEGPV}) = 2.5$, (—); 2.8, (- - -); 3.0, (• • •); 3.1, (— • — • —); 3.3, (- •• - •• - ••); 3.9, (- • - • - •). The latter data were recorded in a separate experiment, hence the different absorbance scale. Arrows indicate the direction of change in the spectra upon adding increasing amounts of TFA.

$\log(n_{TFA}/n_{MTEGPV}) = 2.86$, $[H^+] = 6.66 \times 10^{-3}$ M, pH = 2.18) was identical to the value measured using a calibrated electrode (i.e., pH = 2.19 for this example).

Upon the addition of increasing amounts of TFA to a toluene solution of MTEGPV, the spectral changes observed closely resembled those shown in Figure 1 for DMAPV. For MTEGPV dissolved in water, however, distinct differences were observed in the TFA-dependent absorption spectra (Figure 2). Like the data in toluene, increasing the amount of TFA added to MTEGPV in water caused the absorption band centered at 416 nm to decrease in intensity, while bands in the range ~300−370 nm correspondingly increased in intensity. Moreover, spectra recorded over a large range of added TFA are likewise characterized by the absence of isosbestic points (Figure 2a). However, upon closer examination of the data, it becomes apparent that, at the limit of large amounts of added TFA, the spectra obtained from aqueous solutions of MTEGPV clearly show the existence of isosbestic points at 379 and 288 nm (Figure 2b). Thus, the data shown in Figure 2b strongly suggest that, with large amounts of added TFA in water, one is looking at a TFA concentration-dependent equilibrium between only two species, MTEGPV$-H^+$ and MTEGPV$-H_2^{++}$.

At this juncture, it is important to note that, in both toluene and water, comparatively large amounts of TFA had to be added in order to see appreciable changes in the absorption spectra of

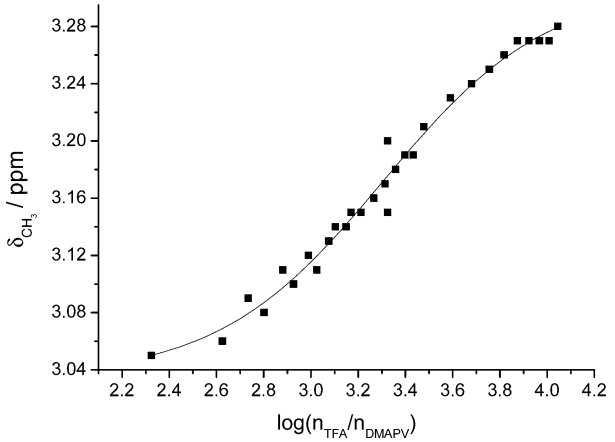

Figure 3. Chemical shift of the protons on the N-substituted methyl groups in DMAPV as a function of the amount of added TFA. The experiment was performed in $CDCl_3$.

DMAPV and MTEGPV, respectively. This is consistent with the expectation that both DMAPV and MTEGPV should be weak bases due to the delocalization of the nitrogen lone pair electrons onto the adjacent π system. To put this point into perspective, recall that an aromatic amine such as aniline has a pK_b of ~9.1.[58] On the other hand, diphenylamine (p$K_b \sim 13.2$)[58] is a weaker base than aniline as a consequence of lone pair delocalization over two adjacent phenyl groups. By extension, pK_b values for the dibasic compound *p*-benzidine (i.e., [1,1′-biphenyl]-4,4′-diamine) are very similar, p$K_b(1) = 9.35$ and p$K_b(2) = 10.57$.[58] This latter point suggests that, upon initial protonation of *p*-benzidine, the molecule twists to effectively decouple the second basic site from the now positively charged conjugate acid at the first site. Similar behavior is observed for the analogous compound 4,4′-diaminostilbene.[59,60] From the data in Figure 2b, assuming that we have an equilibrium between MTEGPV$-H^+$ and MTEGPV$-H_2^{++}$, we estimate that the pK_b value of MTEGPV$-H^+$ is ~11.8, which is consistent with our expectation based on the literature pK_b values mentioned above.

We also note that the spectral changes shown in Figures 1 and 2 were completely reversible upon the addition of $N(CH_3)_3$ to the solutions. In the least, this suggests that acid-catalyzed cis−trans isomerization does not contribute to the changes observed in the absorption spectra. Moreover, for analogous phenylene vinylenes that do not have the terminal-substituted amino groups but, rather, are substituted with alkoxy groups,[9,10] addition of TFA does not cause a change in the absorption spectrum of the compound. Finally, the data shown in Figure 2 were completely reproducible when HCl was used instead of TFA. This indicates that, in the aqueous system, the counterion does not influence the data obtained.

Data recorded from an independent NMR experiment are consistent with protonation of the nitrogen lone pair electrons in these molecules. NMR spectra recorded as a function of TFA added to a solution of DMAPV in chloroform reveal a systematic change in the chemical shift of the protons assigned to the *N*-methyl group (Figure 3). Specifically, with an increase in added TFA, the *N*-methyl resonance shifted further downfield, as expected.[61] It is important to note that, in this experiment in chloroform, a single *N*-methyl resonance was always observed. Thus, on the NMR time scale, protonation−deprotonation is rapid, and one simply observes an average of the species present in the system.

In a simplistic interpretation of the MTEGPV/water data shown in Figure 2, the TFA-dependent disappearance of the absorption band at ~416 nm and the appearance of the "blue-shifted" absorption band at ~350 nm are consistent with the protonation of the amines and the corresponding removal of lone pair electrons from the conjugated π system. As a point of reference, we note that analogous phenylene vinylenes that lack the terminal substituted amino groups have an absorption band with $\lambda_{max} \sim 350-360$ nm,[10] which is consistent with our assignment of the ~350 nm band in Figure 2 to MTEGPV$-H_2^{++}$. Although similar spectral changes are also observed upon the addition of TFA to DMAPV in toluene (Figure 1), the lack of a distinct isosbestic point indicates that this latter system is more complicated. Indeed, for DMAPV solutions already containing TFA, the red shift of the absorption band from ~325 to ~350 nm with an increase in added TFA is not consistent with the expected blue shift associated with successive protonation of the amine moieties. These data may indicate the formation of counterion-mediated aggregates in which intermolecular π overlap occurs between (DMAPV$-H^+$ $^-O_2CCF_3$) or ($CF_3CO_2^-$ $^+H-$DMAPV$-H^+$ $^-O_2CCF_3$) pairs in toluene. The formation of such aggregates, and the associated extension of the π chromophores, could give rise to the observed red shift in the absorption spectra of these ion pairs in a nonpolar solvent.

Support for the interpretation of solvent-promoted aggregation in toluene is available from an additional absorption experiment performed in anisole, which is a more polar solvent than toluene. In contrast to the behavior observed in toluene (Figure 1), addition of TFA to a solution of DMAPV in anisole results in spectral changes that more closely resemble those shown in Figure 2b (MTEGPV in water) where we suggest that aggregate formation does not occur.

Additional insight into the potential formation of TFA-dependent aggregates in the nonpolar solvent is obtained from fluorescence experiments. In the absence of added TFA, the fluorescence spectrum of DMAPV in toluene has a band maximum at ~485 nm with a shoulder at ~525 nm (Figure 4a). Upon the addition of TFA, the fluorescence spectrum changes dramatically. First, we see the appearance of a blue-shifted band centered at ~425 nm. The band appears to be comprised of several vibronic transitions (Figure 4a). This blue-shifted band is consistent with the corresponding TFA-dependent blue shift in the absorption profile of DMAPV (Figure 1) and arguably reflects the shorter chromophore that results upon removal of the lone pair electrons from the π system. Second, and more importantly, we see the appearance of a structureless, red-shifted band with λ_{max} at ~550 nm (Figure 4a). Such a band is not observed upon the addition of TFA to MTEGPV in water (Figure 4b) or upon the addition of TFA to related amino-substituted phenyl vinylenes in ethanol.[22] It seems reasonable to assign this latter red-shifted band to an aggregate of protonated phenylene vinylenes that possibly contains some charge-transfer (CT) character associated with the postulated trifluoroacetate-mediated intermolecular interaction. Within the context of this assignment, it is important to note the lack of a spectral shift in this red-shifted band with a change in the amount of added TFA. As such, "aggregation" may only be limited to the formation of a dimer.

It is also important to note that, at the limit of large amounts of TFA added to the aqueous solutions of MTEGPV, changes in the fluorescence spectra appear to define a common point at ~510 nm (Figure 4b). This correlates with the isosbestic point observed in the MTEGPV absorption experiments (Figure 2b).

Singlet Oxygen Quantum Yields. Upon irradiation at 416 nm, DMAPV dissolved in toluene produces singlet oxygen with a quantum yield of 0.39 ± 0.04. Upon the addition of TFA to solutions of DMAPV in toluene, the quantum yield of singlet

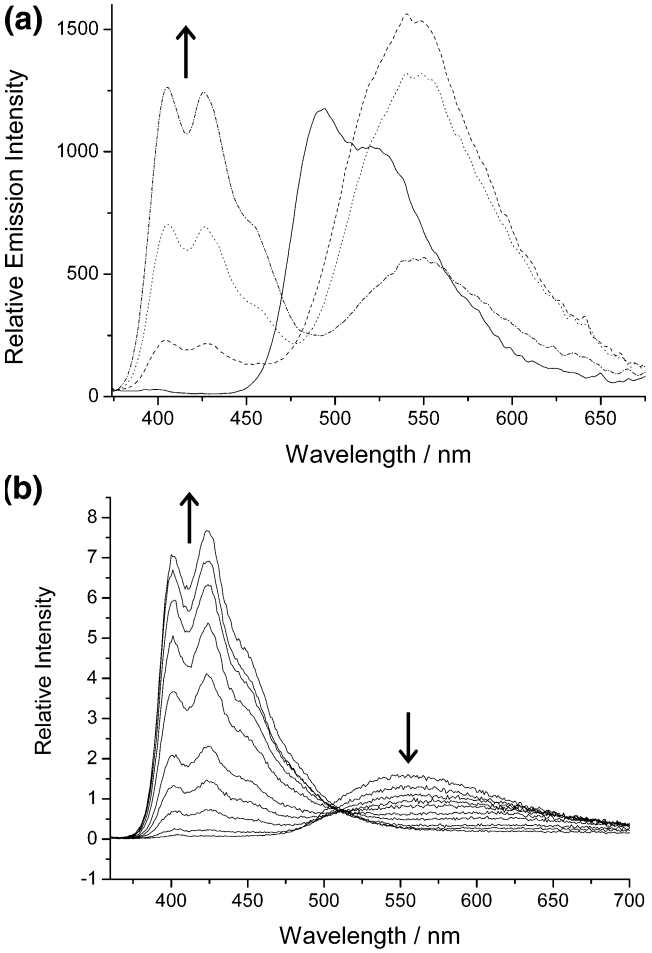

Figure 4. (a) Fluorescence spectra of DMAPV in toluene containing different amounts of trifluoroacetic acid, TFA. The spectra shown reflect different molar ratios of TFA to DMAPV, expressed as $\log(n_{TFA}/n_{DMAPV})$: (—), no TFA; (- - -), 2.5; (• • •), 3.2; (— • — • — •), > 3.5. (b) Fluorescence spectra of MTEGPV in water containing different amounts of TFA, ranging from no TFA to $\log(n_{TFA}/n_{MTEGPV}) > 3.4$. In both cases, sample excitation was at 355 nm, and the data were corrected for differences in absorbance. Arrows indicate the direction of change in the spectra upon adding increasing amounts of TFA.

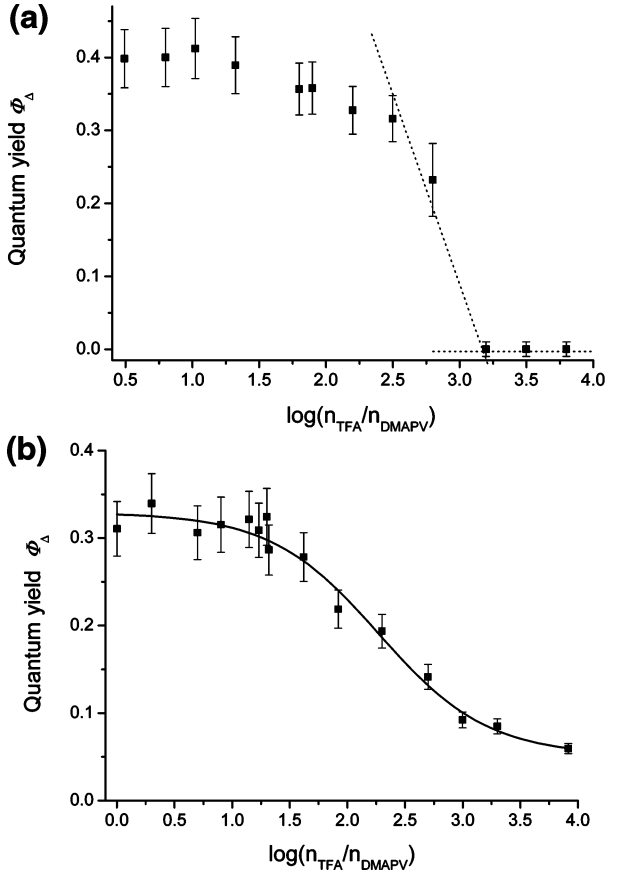

Figure 5. Singlet oxygen quantum yields, Φ_Δ, as a function of the amount of TFA added to a toluene solution of DMAPV, expressed as $\log(n_{TFA}/n_{DMAPV})$. The data were recorded upon (a) 416 nm irradiation and (b) 355 nm irradiation of the system.

oxygen production remains fairly constant over a large range of added TFA before decreasing precipitously to zero (Figure 5a). This behavior is arguably expected from the data shown in Figure 1. Specifically, the only species that absorbs at 416 nm is DMAPV, and upon protonation of DMAPV with sufficiently large amounts of added TFA, this band centered at 416 nm disappears completely. At this limit, singlet oxygen is not produced simply because light is not absorbed.

On the basis of the spectra shown in Figure 1, singlet oxygen quantum yields obtained upon irradiation at 355 nm as a function of TFA added to the DMAPV solution should be of greater interest. At this wavelength, in toluene, the species that absorb light evolve from DMAPV to DMAPV$-H^+$, DMAPV$-H_2^{++}$, and to what we suggest may be aggregates of DMAPV$-H^+$ and DMAPV$-H_2^{++}$. In the absence of added TFA, the singlet oxygen quantum yield observed upon irradiation of DMAPV at 355 nm (0.33 ± 0.04) is, within our margin of error, the same as that obtained upon irradiation at 416 nm. Upon the addition of TFA, however, the quantum yield decreases gradually, ultimately reaching a value of 0.06 ± 0.01 at a significantly large ratio of TFA to DMAPV (Figure 5b). Note that, under these conditions of irradiation at 355 nm, the singlet oxygen quantum yields obtained will reflect a contribution from all species that absorb light at this wavelength (i.e., at a given amount of added TFA, the quantum yield recorded will reflect a weighted average of the quantum yields for the individual species present in solution). In any event, these data clearly indicate that species formed upon protonation of DMAPV in toluene do not produce singlet oxygen as efficiently as the free base, DMAPV.

Upon irradiation of an aqueous solution of MTEGPV at 355 nm, singlet oxygen is produced with a quantum efficiency of 0.09 ± 0.02. Within our error margin, this number is equivalent to our previously published value of 0.11 ± 0.02.[10] To facilitate the ease and accuracy with which we detect singlet oxygen phosphorescence, these experiments were performed in D_2O as opposed to H_2O. (It is acknowledged that the quantum efficiency of singlet oxygen phosphorescence in D_2O is much larger than that in H_2O.[7,51] The use of the deuterated solvent, however, does not influence the singlet oxygen quantum yield.)

Upon adding increasing amounts of TFA to an aqueous solution of MTEGPV, the singlet oxygen quantum yield decreased to a value of zero. Thus, the TFA-dependent behavior of MTEGPV in water resembles that of DMAPV in toluene. In short, the data indicate that the protonated forms of these sensitizers do not produce singlet oxygen as efficiently as the free bases. The data obtained are summarized in Table 1.

To facilitate a better understanding of this system, we examined the effect of other solvents on the quantum efficiency of MTEGPV-sensitized singlet oxygen production. In these experiments, the intensity of the singlet oxygen phosphorescence signal was, once again, used as our probe, and the data obtained were corrected for solvent-dependent changes in the $O_2(a^1\Delta_g)$

TABLE 1: Singlet Oxygen Quantum Yields, Φ_Δ, Sensitizer Triplet State Lifetimes, τ_T, Rate Constants for Oxygen Quenching of the Sensitizer Triplet State, k_q, and the Fractions of Triplet State Sensitizer Quenched by Oxygen, $f_T^{O_2}$ for the Free Base and Protonated Forms of DMAPV and MTEGPV[a]

sensitizer	solvent	$\tau_T^{nitrogen}$ (μs)	τ_T^{air} (μs)	k_q (s^{-1} M^{-1})	$f_T^{O_2}$	Φ_Δ
DMAPV	toluene	2.5 ± 0.2	0.20 ± 0.02	$(2.7 \pm 0.2) \times 10^9$	0.92 ± 0.13	0.33 ± 0.04
DMAPV$-H_2^{++}$	toluene	1.9 ± 0.2	0.20 ± 0.02	$(2.6 \pm 0.2) \times 10^9$	0.89 ± 0.12	0.06 ± 0.01
MTEGPV[b]	toluene	2.9 ± 0.2	0.18 ± 0.01	$(3.1 \pm 0.3) \times 10^9$	0.94 ± 0.08	0.33 ± 0.03
MTEGPV	D_2O	9.1 ± 0.9	3.4 ± 0.3	$(6.6 \pm 0.9) \times 10^8$	0.63 ± 0.08	0.09 ± 0.02
MTEGPV$-H_2^{++}$	D_2O	0.13 ± 0.03	0.13 ± 0.03		0.00 ± 0.02	0.00 ± 0.02

[a] Φ_Δ was determined upon irradiation of the sensitizer at 355 nm. Triplet absorption experiments were performed using both air- and nitrogen-saturated solutions. Values of $f_T^{O_2}$ are for air-saturated solutions. Data for the protonated amino-substituted phenylene vinylenes were obtained under conditions where $\log(n_{TFA}/n_{amine}) > 3.3$. [b] Data for this compound in toluene were obtained from a previous study.[10]

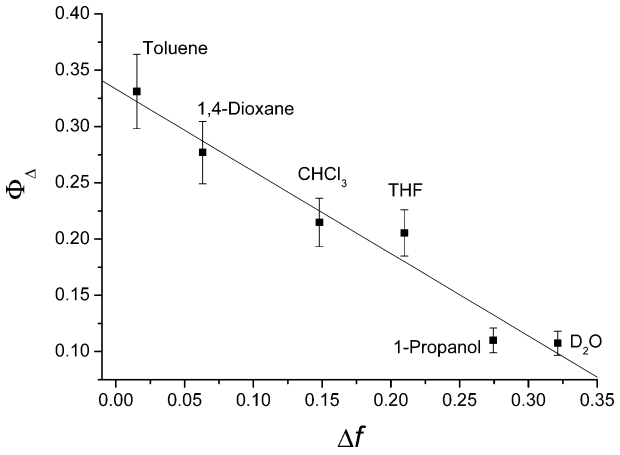

Figure 6. Plot of the MTEGPV-sensitized singlet oxygen quantum yield, Φ_Δ, against the solvent polarity parameter Δf defined in eq 1. For these experiments, MTEGPV was irradiated at 355 nm.

$\rightarrow O_2(X^3\Sigma_g^-)$ radiative rate constant and the extent to which differences in solvent refractive index influence the efficiency of light collection.[54,62]

For this study, we used the reaction field parameter, Δf, that characterizes solvent polarity in terms of its macroscopic static (ϵ_{st}) and optical (ϵ_{op}) dielectric constants (eq 1).[63,64] Note that $\epsilon_{op} = n^2$, where n is the refractive index of that solvent

$$\Delta f = \frac{\epsilon_{st} - 1}{2\epsilon_{st} + 1} - \frac{\epsilon_{op} - 1}{2\epsilon_{op} + 1} \qquad (1)$$

The data obtained indicate that the MTEGPV-sensitized singlet oxygen quantum yield decreases as the solvent polarity increases (Figure 6). These results are consistent with data reported in an earlier study of MTEGPV[10] and, as will be discussed below, point to the importance of CT-mediated processes in the oxygen-dependent photophysics of this sensitizer.

Optical Characterization of the Sensitizer Triplet State. In an attempt to provide an explanation for our TFA-dependent singlet oxygen results, we set out to examine the effect of TFA on the photophysics of the singlet oxygen precursor. From time-resolved fluorescence experiments, we ascertained that the lifetimes of the lowest excited singlet states of DMAPV and MTEGPV, and their protonated derivatives, are all less than 500 ps. We also specifically ascertained that the species responsible for the red-shifted emission band in acidified solutions of DMAPV has a lifetime of 700 ps. With such short lifetimes, one can readily exclude the possibility of sensitizer singlet state deactivation by oxygen quenching. As such, the sole singlet oxygen precursor in these systems must be the lowest energy triplet state of the sensitizer. Thus, it stands to reason that phenomena which perturb the sensitizer triplet state should likewise perturb production of singlet oxygen.

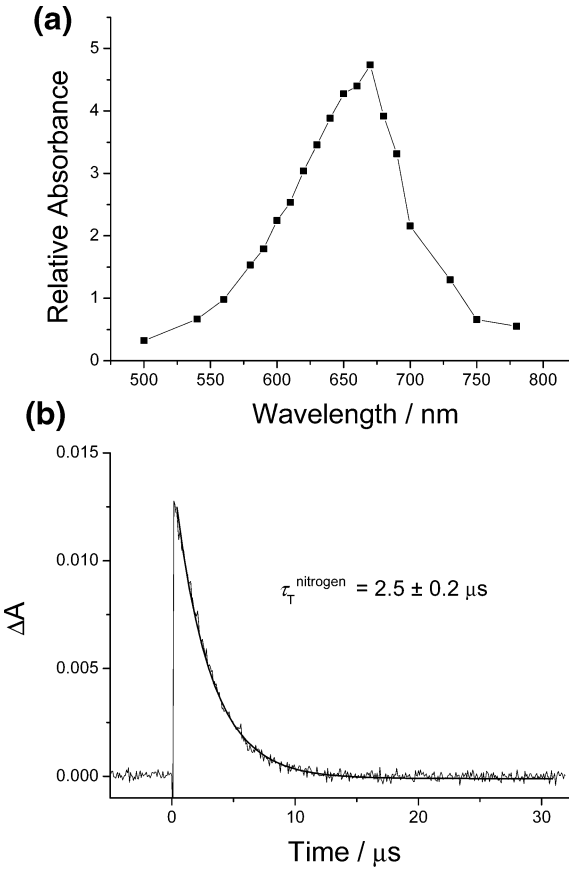

Figure 7. (a) Triplet absorption spectrum and (b) transient signal observed at 670 nm upon 355 nm irradiation of DMAPV in nitrogen-saturated toluene. Superimposed on the decay trace in panel b is the result of a single-exponential fit to the data.

In a time-resolved absorption experiment performed on an oxygen-free, nitrogen-saturated solution of DMAPV in toluene, we observed a transient signal with λ_{max} at 670 nm (Figure 7a). The decay of this signal followed single-exponential kinetics, yielding a lifetime of $\tau = 2.5 \pm 0.2$ μs (Figure 7b). Upon aerating the solution, the lifetime of this transient signal decreased to 200 ± 20 ns. Taking the concentration of oxygen in an air-saturated solution of toluene as 1.7×10^{-3} M,[65] this yields a rate constant of $(2.7 \pm 0.2) \times 10^9$ s^{-1} M^{-1} for oxygen quenching of the transient. These data are consistent with those generally observed from triplet states,[66] and as such, we suggest that this transient absorption signal indeed derives from the DMAPV triplet state.

Upon protonation of DMAPV in toluene to yield DMAPV−H_2^{++} and the putative aggregates (i.e., $\log(n_{TFA}/n_{DMAPV}) > 3$], a transient absorption signal was likewise observed upon 355 nm pulsed-laser irradiation of the system. In this case, however, the spectrum recorded was significantly blue-shifted in comparison to that recorded from DMAPV, with a λ_{max} at 510 nm. In the absence of oxygen, this transient decayed with a lifetime of 1.9 ± 0.2 μs, whereas in an air-saturated solution, a lifetime of 200 ± 20 ns was obtained. In light of the fact that this protonated system may contain more than one species, it is important to note that we still observed single-exponential decay kinetics in these experiments. Moreover, the lifetimes obtained were independent of the probe wavelength within the spectral profile of the transient absorption band. Again, taking the concentration of oxygen in an air-saturated solution of toluene as 1.7×10^{-3} M, these data yield a rate constant of $(2.6 \pm 0.2) \times 10^9$ s^{-1} M^{-1} for oxygen quenching of the transient(s) that gives rise to this absorption signal. On this basis, we likewise suggest that this signal derives from a triplet state.

At this juncture, it is important to note that, in toluene, the rate constant for oxygen quenching of the DMAPV triplet state does not differ significantly from the rate constant for oxygen quenching of the DMAPV−H_2^{++} triplet state (or the triplet state of the putative DMAPV−H_2^{++} aggregate). This result contrasts distinctly with that reported for methylene blue in aqueous solutions, where protonation of the dye molecule led to a pronounced decrease in the rate constant for triplet state quenching by oxygen (vide supra).[34]

We performed analogous time-resolved absorption experiments on aqueous solutions of MTEGPV. In examining these data (Table 1), it is important to recall that the concentration of oxygen in air-saturated water ($\sim 2.8 \times 10^{-4}$ M) is significantly less than that in air-saturated toluene ($\sim 1.7 \times 10^{-3}$ M).[65] Thus, our data indicate that the rate constant for oxygen quenching of the MTEGPV triplet state in water (6.6×10^8 s^{-1} M^{-1}) is not as large as that for the MTEGPV triplet state in toluene (3.1×10^9 s^{-1} M^{-1})[10] or for the DMAPV triplet state in toluene (2.7×10^9 s^{-1} M^{-1}). Second, the data indicate that protonation of MTEGPV to yield MTEGPV−H_2^{++} appreciably shortens the lifetime of the transient assigned to the triplet state. This latter behavior contrasts with that observed upon protonation of DMAPV in toluene (Table 1). We will return to these points as our discussion evolves.

Before progressing further, however, it is useful to consider the kinetic model of our photosystem shown in Scheme 2. On this basis and for the case where the sole singlet oxygen precursor is the sensitizer triplet state, T_1, the quantum yield of singlet oxygen production, Φ_Δ, is expressed as the product of three terms: the quantum yield of triplet state production, Φ_T, the fraction of triplet states quenched by ground state oxygen, $f_T^{O_2}$, and the fraction of such quenching events that result in the production of singlet oxygen, S_Δ (eq 2)

$$\Phi_\Delta = \Phi_T f_T^{O_2} S_\Delta \quad (2)$$

As can be deduced from the expressions in Scheme 2, values of $f_T^{O_2}$ can be readily determined from triplet state lifetimes obtained from experiments performed using N_2- and air-saturated solutions, and these values are shown in Table 1. The results clearly indicate that, for DMAPV and DMAPV−H_2^{++} in toluene, almost all of the triplet states produced are quenched by oxygen. Thus, the pronounced change in Φ_Δ for this sensitizer upon the addition of TFA to the solution must derive from protonation-dependent changes in Φ_T and/or S_Δ. We will return to this point shortly.

SCHEME 2: A Kinetic Model for the Photosensitized Production of Singlet Oxygen[a]

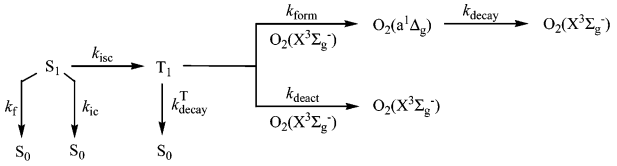

$\tau_T^{nitrogen} = \frac{1}{k_{decay}^T}$ is the inherent, oxygen-independent lifetime of the triplet state

$\tau_T^{air} = \frac{1}{k_{decay}^T + k_q [O_2(X^3\Sigma_g^-)]}$ is the triplet state lifetime in the presence of oxygen

$k_q = k_{form} + k_{deact}$ is the overall rate constant for $O_2(X^3\Sigma_g^-)$ quenching of the triplet state

$f_T^{O_2} = \frac{k_q [O_2(X^3\Sigma_g^-)]}{k_q [O_2(X^3\Sigma_g^-)] + k_{decay}^T}$ is the fraction of triplet states quenched by $O_2(X^3\Sigma_g^-)$

$S_\Delta = \frac{k_{form}}{k_{form} + k_{deact}}$ is the fraction of O_2 quenching events that result in $O_2(a^1\Delta_g)$

k_f, k_{ic}, and k_{isc} are rate constants for fluorescence, internal conversion, and intersystem crossing

[a] S_0, S_1, and T_1 denote the ground state, first excited singlet state, and first excited triplet state, respectively, of the sensitizer.

For MTEGPV dissolved in water, a significant fraction of the triplet states produced are also quenched by oxygen ($f_T^{O_2} = 0.63$). However, the quantum yield of MTEGPV-sensitized singlet oxygen production in water ($\Phi_\Delta = 0.09$) is significantly smaller than that from either MTEGPV or DMAPV dissolved in toluene ($\Phi_\Delta = 0.33$, Table 1). In this case, the data indicate that solvent-dependent changes in Φ_T and/or S_Δ likewise play a more pronounced role than $f_T^{O_2}$ in establishing the magnitude of Φ_Δ. As we have already mentioned, the data in Figure 6 as well as data from an independent study[10] implicate the importance of oxygen-dependent CT-mediated processes in this phenomenon. Again, we will return to this point shortly.

Upon protonation of MTEGPV in water, it is clear that an oxygen-independent mechanism for facile triplet state deactivation becomes possible. Under these conditions, where the lifetime of the MTEGPV−H_2^{++} triplet state is quite short, bimolecular quenching by oxygen is not a competitive channel for triplet state deactivation, and $f_T^{O_2}$ is zero. Although the latter readily explains why Φ_Δ is likewise zero in this case, we must also consider the more fundamental point that the protonation-dependent change in the lifetime of the MTEGPV triplet state may reflect the same phenomenon that also influences S_Δ, for example, in the DMAPV system (vide infra).

Optoacoustic Characterization of the Photosystem. We now comment on the other two parameters in eq 2 that influence the yield of singlet oxygen production in our photosensitized process, Φ_T and S_Δ. To this end and to support the transient absorption experiments, time-resolved LIOAC measurements were performed to quantify the heat released from the DMAPV system under a variety of conditions.

In a LIOAC experiment on a given compound, one can quantify the fraction of "fast" heat released, α, and distinguish this from heat released over longer periods of time (i.e., "slow" heat release).[67,68] Briefly, fast heat is attributed to heat released on time scales shorter than the effective acoustic transit time, τ_a. The latter is obtained from the expression $\tau_a = d/v_s$, where d is the diameter of the laser beam and v_s is the speed of sound in the given medium.[12,68] In our LIOAC experiments on DMAPV and DMAPV−H_2^{++}, the diameter of the laser beam used to irradiate the system at 355 nm was adjusted such that

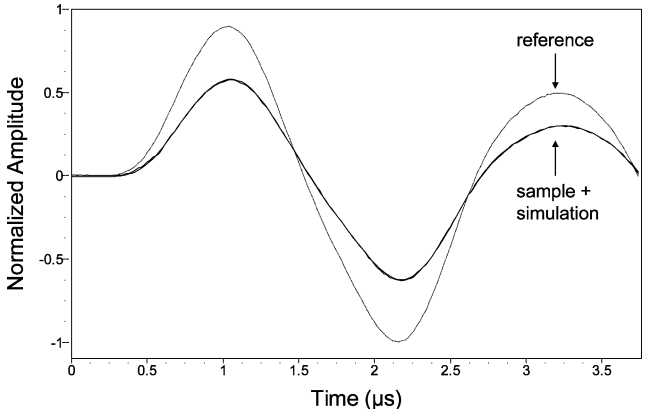

Figure 8. LIOAC signal observed subsequent to 355 nm pulsed-laser irradiation of DMAPV in nitrogen-saturated toluene and, independently, the signal observed from the reference used to calibrate heat release, 2-hydroxybenzophenone. Superimposed on, and indistinguishable from, the data from DMAPV is a simulation obtained using a time constant for fast heat release of 500 ps and a time constant for slow heat release of 2.5 μs (residuals were <1%).

$\tau_a \sim 200$ ns. For experiments performed in the absence of oxygen, as in our case, fast heat release derives from deactivation of the sensitizer singlet excited states, whereas slow heat release reflects deactivation of the lowest energy triplet state, T_1. In practice, values of α are obtained from a relative experiment performed against a calibrated calorimetric standard. For our experiments, the standard was 2-hydroxybenzophenone, which releases all of its excitation energy as fast heat (i.e., $\alpha = 1$).[68,69]

Upon irradiation at 355 nm, the amplitudes of the waveforms obtained in LIOAC experiments yielded $\alpha = 0.61 \pm 0.03$ for DMAPV and 0.53 ± 0.02 for DMAPV$-H_2^{++}$. Independent confirmation of these values was obtained in a numerical simulation of the time-resolved acoustic waveform (Figure 8). For this latter exercise, a time constant for fast heat release of 500 ps was used to characterize the rate of singlet state deactivation. To characterize the rate of slow heat release, we used a time constant of 2.5 μs for DMAPV and 1.9 μs for DMAPV$-H_2^{++}$, as obtained from our time-resolved absorption experiments (Table 1). From these simulations, we obtained $\alpha = 0.62$ for DMAPV and 0.54 for DMAPV$-H_2^{++}$, in good agreement with the data obtained from the waveform amplitudes.

Recognizing that the molar energy, E_L, deposited into the system by the pulsed laser is known and that energy must be conserved, we can write an expression such as that shown in eq 3[68]

$$E_L(1-\alpha) = \Phi_F E_F^{BandMax} + \Phi_T E_T \exp\left(-\frac{\tau_a}{\tau_T^{nitrogen}}\right) \quad (3)$$

In independent fluorescence experiments, we determined the quantum yields of fluorescence, Φ_F, from both DMAPV and DMAPV$-H_2^{++}$ by comparing the intensity of emitted light to that emitted from a standard molecule (9,10-diphenylanthracene in cyclohexane). Values for the energy of the fluorescent state were obtained both from the peak maximum of the fluorescence spectral profile, $E_F^{BandMax}$, and from the crossing point of the intensity-normalized absorption and fluorescence spectra, $E_F^{0,0}$. Data obtained in these measurements are shown in Table 2.

Using the values of α obtained in the LIOAC experiment, along with the appropriate values of E_L for 355 nm excitation (i.e., 337 kJ/mol) and $\Phi_F E_F^{BandMax}$ (Table 2), we obtain $\Phi_T E_T = 89 \pm 10$ and 73 ± 8 kJ/mol for DMAPV and DMAPV$-H_2^{++}$, respectively, through eq 3.

Effect of Protonation on the Singlet Oxygen Precursor. We first consider the values for $\Phi_T E_T$ obtained through the use of eq 3. For DMAPV, we obtained $\Phi_T E_T = 89 \pm 10$ kJ/mol. Recognizing that Φ_F for DMAPV is 0.20 ± 0.02 (Table 2), then Φ_T can be no larger than 0.80, and E_T can be no smaller than 111 ± 13 kJ/mol. Note that the excitation energy of singlet oxygen is 94 kJ/mol. Similarly, we ascertain that E_T for DMAPV$-H_2^{++}$ can be no smaller than 106 ± 12 kJ/mol. Admittedly, the propagated errors on these lower limits for E_T are large. Nevertheless, if we assume that the sources of the errors are the same, then it is meaningful to see that the estimated lower limit for E_T in DMAPV is essentially the same as that for E_T in DMAPV$-H_2^{++}$. In short, the data indicate that there is not a pronounced protonation-dependent change in E_T for these molecules. Thus, it appears that protonation-dependent changes in Φ_Δ for this system do not reflect a value of E_T in DMAPV$-H_2^{++}$ that falls below the energetic threshold of 94 kJ/mol required for singlet oxygen excitation.

Of course, if E_T does not vary significantly upon protonation or if it increases only slightly, as is the case with the energy of the singlet state (Table 2), then the observed blue shift in the triplet absorption spectrum upon protonation must principally reflect a change in the energy level of a higher-lying triplet state.

Making use of eq 2 and the experimentally obtained values of $f_T^{O_2}$, Φ_Δ, and $\Phi_T E_T$ for DMAPV and DMAPV$-H_2^{++}$ in toluene (Tables 1 and 2), one can readily arrive at the expression shown in eq 4

$$\frac{S_\Delta^{DMAPV}}{S_\Delta^{DMAPV-H_2^{++}}} = (4.4 \pm 1.4)\frac{E_T^{DMAPV}}{E_T^{DMAPV-H_2^{++}}} \quad (4)$$

If, as we have argued, there is not a significant change in the value of E_T upon protonation, then our data indicate that there is an appreciable protonation-dependent change in the fraction of triplet states quenched by oxygen that yield singlet oxygen (i.e., $S_\Delta^{DMAPV} > S_\Delta^{DMAPV-H_2^{++}}$). In short, it is this term in eq 2 that principally defines the protonation-dependent changes in the singlet oxygen quantum yield for this sensitizer in toluene.

Mechanistic Considerations. There is sufficient evidence in the literature to indicate that an increase in the amount of CT character, both within a given sensitizer and in the sensitizer−oxygen encounter complex, adversely affects the yield of singlet oxygen production.[7,70−73] This increase in the amount of CT character is often discussed in terms of an increase in the extent to which the ^{1,3}(Sensitizer$^{+\bullet}-O_2^{-\bullet}$) states mix with lower-lying valence states of the encounter complex (e.g., $T_1-O_2(X^3\Sigma_g^-)$, $S_0-O_2(a^1\Delta_g)$, and $S_0-O_2(X^3\Sigma_g^-)$].[52,74,75] In cases that promote more CT character (e.g., polar solvents and sensitizers with a low oxidation potential), the decrease in the singlet oxygen yield is generally attributed to an increase in the probability of CT-mediated radiationless processes that deactivate the excited-state sensitizer (i.e., $T_1-O_2(X^3\Sigma_g^-) \rightarrow S_0-O_2(X^3\Sigma_g^-)$] and that operate at the expense of the energy-transfer process to produce singlet oxygen. This phenomenon is directly manifested in the magnitude of S_Δ.

We have already established through studies on solvent and substituent effects that, as singlet oxygen sensitizers, the phenylene vinylene systems examined in the present study are susceptible to CT effects.[9,10] This conclusion is reinforced by the data shown in Figure 6. By extension, it stands to reason

TABLE 2: Quantum Yields of Fluorescence, Φ_F, Fluorescent State Energy, E_F, Fraction of Heat Released as Fast Heat, α, and the Product, $\Phi_T E_T$, for the DMAPV System in Toluene[a]

molecule	Φ_F	$E_F^{BandMax}$ (kJ mol^{-1})	$E_F^{0,0}$ (kJ mol^{-1})	α	$\Phi_T E_T$ (kJ mol^{-1})
DMAPV	0.20 ± 0.02	245 ± 1	256 ± 2	0.61 ± 0.03	89 ± 10
DMAPV−H_2^{++}	0.31 ± 0.03	298 ± 1	306 ± 3	0.53 ± 0.02	73 ± 8

[a] Values of $\Phi_T E_T$ were determined using eq 3 with E_L = 337 kJ mol^{-1}. Data for the protonated amino-substituted phenylene vinylene were obtained under conditions where $\log(n_{TFA}/n_{amine}) > 3.3$. In the presence of TFA, E_F was obtained from the "blue-shifted" fluorescence band (see Figure 4a). Values of Φ_F were obtained by integrating over the entire spectral profile of emission, including the "red-shifted" band (see Figure 4a).

that CT effects may likewise be involved upon protonation of the sensitizer and, in turn, also manifested in the magnitude of S_Δ.

Although aspects of our present data from these phenylene vinylene systems are in keeping with this CT-based model, there are, nevertheless, specific features of this system that deserve comment and, ultimately, additional study. First, even in the absence of oxygen, protonation of MTEGPV to yield MTEGPV−H_2^{++} appreciably shortens the lifetime of the triplet state. Similar behavior was not observed for DMAPV in toluene (Table 1). It is possible that such behavior with MTEGPV in water could partly reflect a solvent-enhanced increase in an intramolecular CT-mediated deactivation channel.[73,76−78] In support of this interpretation, we note that, in toluene, Φ_F(MTEGPV) = 0.16 ± 0.02, whereas in water, Φ_F(MTEGPV) = 0.040 ± 0.004.[10] Alternatively, the proton-facilitated deactivation of the sensitizer triplet state in water could be envisioned as the logical consequence of the facile equilibrium involving the protonation and deprotonation of electrons in the chromophore; the proton-dependent "movement" of electrons in the chromophore, coupled to the movement of the proton itself, provides an effective channel for radiationless deactivation. A similar phenomenon is seen in the deactivation of *o*-hydroxybenzophenones, for example, where a facile keto−enol tautomerization promotes radiationless deactivation.[79] Such coupling to nuclear translational degrees of freedom may not be as pronounced in toluene where the (DMAPV−H^+ $^-O_2CCF_3$) or ($CF_3CO_2^-$ $^+$H−DMAPV−H^+ $^-O_2CCF_3$) ion pairs are arguably more static. Indeed, the fluorescence quantum yield increases upon the addition of TFA to a solution of DMAPV in toluene (Table 2), which is consistent with the picture of a comparatively static ion pair (or aggregate of ion pairs). However, we must be somewhat circumspect with respect to this latter point in that the fluorescence quantum yield of MTEGPV in water, although small, likewise increases upon protonation [Φ_F(MTEGPV) = 0.04, Φ_F (MTEGPV−H_2^{++}) = 0.08], as does the fluorescence quantum yield of a related amino-substituted phenylene vinylene upon protonation in ethanol.[22]

Second, the rate constant for oxygen quenching of the MTEGPV triplet state in water (6.6×10^8 s^{-1} M^{-1}) is appreciably smaller than that for oxygen quenching of the MTEGPV triplet state in toluene (3.1×10^9 s^{-1} M^{-1}). Likewise, this could reflect a solvent-dependent change in the extent to which the MTEGPV−O_2 CT state mixes with lower-lying valence states of the MTEGPV−O_2 encounter complex. There is certainly ample precedence in the literature to demonstrate that changes in the extent of CT character in a given oxygen−organic molecule complex can indeed be manifested in the rate constant for oxygen quenching of the organic molecule excited state.[80,81] On the other hand, the implication is that CT effects should be more pronounced in water than in toluene (e.g., data in Figure 6), and for a CT-mediated process, one would expect the rate constant for oxygen quenching of the MTEGPV triplet state to be larger in water than in toluene. Thus, in this specific case, it appears that CT effects may not play as large of a role as we might otherwise expect. In any event, the observation that k_q^{MTEGPV}(toluene) > k_q^{MTEGPV}(H_2O) is an issue that also requires further investigation.

Finally, it is important to recall that protonation of DMAPV in toluene does not change the magnitude of the rate constant for oxygen quenching of the triplet state, despite the fact that we observe a pronounced protonation-dependent change in Φ_Δ. These data may indicate that, in toluene, the putative protonation-dependent phenomenon of aggregation may, in fact, play a more important role than charge transfer in influencing the yield of singlet oxygen. Again, recall that sensitizer aggregation is known to result in decreased yields of singlet oxygen.[28]

Conclusions

We have demonstrated that protonation of a photosensitizer can significantly affect properties of the system that, in turn, influence the production of singlet oxygen. For the particular system studied, we specifically ascertained that protonation can decrease the efficiency with which singlet oxygen is produced upon oxygen quenching of the sensitizer triplet state (i.e., $S_\Delta^{free\ base} > S_\Delta^{protonated}$). In light of previous studies on other molecules where protonation-dependent changes in the quantum yield of photosensitized singlet oxygen production have been ascribed to changes in the quantum yield of the triplet state sensitizer, Φ_T, and to possible changes in the triplet state energy, E_T, our results demonstrate that this photosystem can respond to protonation in other ways. Perhaps more importantly, our study indicates that an apparently simple system can actually be quite complicated, and further work will be necessary to more completely elucidate the ramifications of sensitizer protonation.

The issues discussed in this report are seen to be particularly relevant for sensitizers whose pK_b values coincide with a pH gradient in the surrounding microenvironment, many examples of which can be found in biological systems. As such, the quantum yield of singlet oxygen production reported for a given sensitizer based on bulk solution-phase measurements may not necessarily be applicable for that sensitizer in vivo. Finally, the issues addressed in this report are likewise important in the development and use of sensitizers for the emerging fields of both one- and two-photon initiated imaging experiments of singlet oxygen in biological samples.[19−21]

Acknowledgment. This work was supported by the Danish National Research Foundation through a block grant for the Center for Oxygen Microscopy and Imaging.

References and Notes

(1) Foote, C. S.; Clennan, E. L. In *Active Oxygen in Chemistry*; Foote, C. S., Valentine, J. S., Greenberg, A., Liebman, J. F., Eds.; Chapman and Hall: London, 1995; pp 105−140.

(2) Ledford, H. K.; Niyogi, K. K. *Plant Cell Environ.* **2005**, *28*, 1037−1045.

(3) op den Camp, R. G. L.; Przybyla, D.; Ochsenbein, C.; Laloi, C.; Kim, C.; Danon, A.; Wagner, D.; Hideg, E.; Göbel, C.; Feussner, I.; Nater, M.; Apel, K. *Plant Cell* **2003**, *15*, 2320−2332.

(4) Ryter, S. W.; Tyrrell, R. M. *Free Radical Biol. Med.* **1998**, *24*, 1520−1534.

(5) Kochevar, I. E.; Lynch, M. C.; Zhuang, S.; Lambert, C. R. *Photochem. Photobiol.* **2000**, *72*, 548−553.

(6) Dougherty, T. J.; Gomer, C. J.; Henderson, B. W.; Jori, G.; Kessel, D.; Korbelik, M.; Moan, J.; Peng, Q. *J. Natl. Cancer Inst.* **1998**, *90*, 889−905.

(7) Schweitzer, C.; Schmidt, R. *Chem. Rev.* **2003**, *103*, 1685−1757.

(8) Frederiksen, P. K.; Jørgensen, M.; Ogilby, P. R. *J. Am. Chem. Soc.* **2001**, *123*, 1215−1221.

(9) Frederiksen, P. K.; McIlroy, S. P.; Nielsen, C. B.; Nikolajsen, L.; Skovsen, E.; Jørgensen, M.; Mikkelsen, K. V.; Ogilby, P. R. *J. Am. Chem. Soc.* **2005**, *127*, 255−269.

(10) Nielsen, C. B.; Johnsen, M.; Arnbjerg, J.; Pittelkow, M.; McIlroy, S. P.; Ogilby, P. R.; Jørgensen, M. *J. Org. Chem.* **2005**, *70*, 7065−7079.

(11) Poulsen, T. D.; Frederiksen, P. K.; Jørgensen, M.; Mikkelsen, K. V.; Ogilby, P. R. *J. Phys. Chem. A* **2001**, *105*, 11488−11495.

(12) Arnbjerg, J.; Johnsen, M.; Frederiksen, P. K.; Braslavsky, S. E.; Ogilby, P. R. *J. Phys. Chem. A* **2006**, *110*, 7375−7385.

(13) Karotki, A.; Kruk, M.; Drobizhev, M.; Rebane, A.; Nickel, E.; Spangler, C. W. *IEEE J. Quantum Electron.* **2001**, *7*, 971−975.

(14) Oar, M. A.; Serin, J. M.; Dichtel, W. R.; Fréchet, J. M. J.; Ohulchanskyy, T. Y.; Prasad, P. N. *Chem. Mater.* **2005**, *17*, 2267−2275.

(15) Rumi, M.; Ehrlich, J. E.; Heikal, A. A.; Perry, J. W.; Barlow, S.; Hu, Z.; McCord-Maughon, D.; Parker, T. C.; Röckel, H.; Thayumanavan, S.; Marder, S. R.; Beljonne, D.; Brédas, J.-L. *J. Am. Chem. Soc.* **2000**, *122*, 9500−9510.

(16) Reinhardt, B. A.; Brott, L. L.; Clarson, S. J.; Dillard, A. G.; Bhatt, J. C.; Kannan, R.; Yuan, L.; He, G. S.; Prasad, P. N. *Chem. Mater.* **1998**, *10*, 1863−1874.

(17) Strehmel, B.; Sarker, A. M.; Detert, H. *ChemPhysChem* **2003**, *4*, 249−259.

(18) Albota, M.; Beljonne, D.; Brédas, J.-L.; Ehrlich, J. E.; Fu, J.-Y.; Heikal, A. A.; Hess, S. E.; Kogej, T.; Levin, M. D.; Marder, S. R.; McCord-Maughon, D.; Perry, J. W.; Röckel, H.; Rumi, M.; Subramaniam, G.; Webb, W. W.; Wu, X.-L.; Xu, C. *Science* **1998**, *281*, 1653−1656.

(19) Snyder, J. W.; Zebger, I.; Gao, Z.; Poulsen, L.; Frederiksen, P. K.; Skovsen, E.; McIlroy, S. P.; Klinger, M.; Andersen, L. K.; Ogilby, P. R. *Acc. Chem. Res.* **2004**, *37*, 894−901.

(20) Snyder, J. W.; Skovsen, E.; Lambert, J. D. C.; Poulsen, L.; Ogilby, P. R. *Phys. Chem. Chem. Phys.* **2006**, *8*, 4280−4293.

(21) Skovsen, E.; Snyder, J. W.; Ogilby, P. R. *Photochem. Photobiol.* **2006**, *82*, 1187−1197.

(22) Werts, M. H. V.; Gmouh, S.; Mongin, O.; Pons, T.; Blanchard-Desce, M. *J. Am. Chem. Soc.* **2004**, *126*, 16294−16295.

(23) Moan, J.; Smedshammer, L.; Christensen, T. *Cancer Lett.* **1980**, *9*, 327−332.

(24) Brault, D. *J. Photochem. Photobiol., B* **1990**, *6*, 79−86.

(25) Bellnier, D. A.; Young, D. N.; Detty, M. R.; Camacho, S. H.; Oseroff, A. R. *Photochem. Photobiol.* **1999**, *70*, 630−636.

(26) Kubát, P.; Lang, K.; Anzenbacher, P. *Biochim. Biophys. Acta* **2004**, *1670*, 40−48.

(27) Vakrat-Haglili, Y.; Weiner, L.; Brumfeld, V.; Brandis, A.; Salomon, Y.; McIlroy, B.; Wilson, B. C.; Pawlak, A.; Rozanowska, M.; Sarna, T.; Scherz, A. *J. Am. Chem. Soc.* **2005**, *127*, 6487−6497.

(28) Tanielian, C.; Schweitzer, C.; Mechin, R.; Wolff, C. *Free Radical Biol. Med.* **2001**, *30*, 208−212.

(29) Oleinick, N. L.; Morris, R. L.; Belichenko, I. *Photochem. Photobiol. Sci.* **2002**, *1*, 1−21.

(30) Alberts, B.; Johnson, A.; Lewis, J.; Raff, M.; Roberts, K.; Walter, P. *Molecular Biology of the Cell*; Garland Science: New York, 2002.

(31) Stubbs, M.; McSheehy, P. M. J.; Griffiths, J. R.; Bashford, C. L. *Mol. Med. Today* **2000**, *6*, 15−19.

(32) Vaupel, P.; Kallinowski, F.; Okunieff, P. *Cancer Res.* **1989**, *49*, 6449−6465.

(33) Kozin, S. V.; Shkarin, P.; Gerweck, L. E. *Cancer Res.* **2001**, *61*, 4740−4743.

(34) Bonneau, R.; Pottier, R.; Bagno, O.; Joussot-Dubien, J. *Photochem. Photobiol.* **1975**, *21*, 159−163.

(35) Pottier, R.; Bonneau, R.; Joussot-Dubien, J. *Photochem. Photobiol.* **1975**, *22*, 59−61.

(36) Bagno, O.; Soulignac, J. C.; Joussot-Dubien, J. *Photochem. Photobiol.* **1979**, *29*, 1079−1081.

(37) Beeby, A.; FitzGerald, S.; Stanley, C. F. *J. Chem. Soc., Perkin Trans. 2* **2001**, 1978−1982.

(38) Ogunsipe, A.; Nyokong, T. *J. Mol. Struct.* **2004**, *689*, 89−97.

(39) Gensch, T.; Viappiani, C.; Braslavsky, S. E. *J. Am. Chem. Soc.* **1999**, *121*, 10573−10582.

(40) Kruk, M. M.; Braslavsky, S. E. *J. Phys. Chem. A* **2006**, *110*, 3414−3425.

(41) Ostler, R. B.; Scully, A. D.; Taylor, A. G.; Gould, I. R.; Smith, T. A.; Waite, A.; Phillips, D. *Photochem. Photobiol.* **2000**, *71*, 397−404.

(42) Dumas, S.; Leprêtre, J.-C.; Lepellec, A.; Darmanyan, A.; Jardon, P. *J. Photochem. Photobiol., A* **2004**, *163*, 297−306.

(43) Ehrenberg, B.; Anderson, J. L.; Foote, C. S. *Photochem. Photobiol.* **1998**, *68*, 135−140.

(44) Thomas, A. H.; Lorente, C.; Capparelli, A. L.; Martinez, C. G.; Braun, A. M.; Oliveros, E. *Photochem. Photobiol. Sci.* **2003**, *2*, 245−250.

(45) Lorente, C.; Thomas, A. H. *Acc. Chem. Res.* **2006**, *39*, 395−402.

(46) McDonnell, S. O.; Hall, M. J.; Allen, L. T.; Byrne, A.; Gallagher, W. M.; O'Shea, D. F. *J. Am. Chem. Soc.* **2005**, *127*, 16360−16361.

(47) de la Peña, D.; Marti, C.; Nonell, S.; Martinez, L. A.; Miranda, M. A. *Photochem. Photobiol.* **1997**, *65*, 828−832.

(48) Rougee, M.; Bensasson, R. V.; Land, E. J.; Pariente, R. *Photochem. Photobiol.* **1988**, *47*, 485−489.

(49) Scurlock, R.; Rougee, M.; Bensasson, R. V. *Free Radical Res. Commun.* **1990**, *8*, 251−258.

(50) Bisby, R. H.; Morgan, C. G.; Hamblett, I.; Gorman, A. A. *J. Phys. Chem. A* **1999**, *103*, 7454−7459.

(51) Ogilby, P. R. *Acc. Chem. Res.* **1999**, *32*, 512−519.

(52) Paterson, M. J.; Christiansen, O.; Jensen, F.; Ogilby, P. R. *Photochem. Photobiol.* **2006**, *82*, 1136−1160.

(53) Meech, S. R.; Phillips, D. *J. Photochem.* **1983**, *23*, 193−217.

(54) Scurlock, R. D.; Nonell, S.; Braslavsky, S. E.; Ogilby, P. R. *J. Phys. Chem.* **1995**, *99*, 3521−3526.

(55) Schmidt, R.; Tanielian, C.; Dunsbach, R.; Wolff, C. *J. Photochem. Photobiol., A* **1994**, *79*, 11−17.

(56) Marti, C.; Jürgens, O.; Cuenca, O.; Casals, M.; Nonell, S. *J. Photochem. Photobiol., A* **1996**, *97*, 11−18.

(57) Blum, J.; Zimmerman, M. *Tetrahedron* **1972**, *28*, 275−280.

(58) Lide, D. R., Ed. *Handbook of Chemistry and Physics*, 82nd ed.; CRC Press: Boca Raton, FL, 2001.

(59) Smit, K. J.; Ghiggino, K. P. *Chem. Phys. Lett.* **1985**, *122*, 369−374.

(60) Smit, K. J.; Ghiggino, K. P. *J. Photochem.* **1986**, *34*, 23−34.

(61) Dyer, J. R. *Applications of Absorption Spectroscopy of Organic Compounds*; Prentice Hall: Englewood Cliffs, NJ, 1965.

(62) Scurlock, R. D.; Ogilby, P. R. *J. Phys. Chem.* **1987**, *91*, 4599−4602.

(63) Billing, G. D.; Mikkelsen, K. V. *Introduction to Molecular Dynamics and Chemical Kinetics*; Wiley: New York, 1996.

(64) Birks, J. B. *Photophysics of Aromatic Molecules*; Wiley-Interscience: London, 1970.

(65) Battino, R., Ed. *IUPAC Solubility Data Series. Volume 7: Oxygen and Ozone*; Pergamon Press: Oxford, U.K., 1981.

(66) Murov, S. L.; Carmichael, I.; Hug, G. L. *Handbook of Photochemistry*, 2nd ed.; Marcel Dekker: New York, 1993.

(67) Heihoff, K.; Redmond, R. W.; Braslavsky, S. E.; Rougee, M.; Salet, C.; Favre, A.; Bensasson, R. V. *Photochem. Photobiol.* **1990**, *51*, 635−641.

(68) Braslavsky, S. E.; Heibel, G. E. *Chem. Rev.* **1992**, *92*, 1381−1410.

(69) Van Haver, P.; Viaene, L.; Van Der Auweraer, M.; De Schryver, F. C. *J. Photochem. Photobiol., A* **1992**, *63*, 265−277.

(70) Kristiansen, M.; Scurlock, R. D.; Iu, K.-K.; Ogilby, P. R. *J. Phys. Chem.* **1991**, *95*, 5190−5197.

(71) McGarvey, D. J.; Szekeres, P. G.; Wilkinson, F. *Chem. Phys. Lett.* **1992**, *199*, 314−319.

(72) Schmidt, R.; Shafii, F.; Schweitzer, C.; Abdel-Shafi, A. A.; Wilkinson, F. *J. Phys. Chem. A* **2001**, *105*, 1811−1817.

(73) Flors, C.; Ogilby, P. R.; Luis, J. G.; Grillo, T. A.; Izquierdo, L. R.; Gentili, P.-L.; Bussotti, L.; Nonell, S. *Photochem. Photobiol.* **2006**, *82*, 95−103.

(74) Ogilby, P. R.; Sanetra, J. *J. Phys. Chem.* **1993**, *97*, 4689−4694.

(75) Kawaoka, K.; Khan, A. U.; Kearns, D. R. *J. Chem. Phys.* **1967**, *46*, 1842−1853.

(76) Michl, J.; Bonačić-Koutecký, V. *Electronic Aspects of Organic Photochemistry*; Wiley-Interscience: New York, 1990.

(77) Mulliken, R. S.; Person, W. B. *Molecular Complexes*; Wiley: New York, 1969.

(78) Il'ichev, Y. V.; Kühnle, W.; Zachariasse, K. A. *Chem. Phys.* **1996**, *211*, 441−453.

(79) Hou, S.-H.; Hetherington, W. M.; Korenowski, G. M.; Eisenthal, K. B. *Chem. Phys. Lett.* **1979**, *68*, 282−284.

(80) Kikuchi, K.; Sato, C.; Watabe, M.; Ikeda, H.; Takahashi, Y.; Miyashi, T. *J. Am. Chem. Soc.* **1993**, *115*, 5180−5184.

(81) Abdel-Shafi, A. A.; Wilkinson, F. *Phys. Chem. Chem. Phys.* **2002**, *4*, 248−254.